**Proceedings of the ASME 2014 International Design Engineering Technical Conferences &
Smart Materials, Adaptive Structures and Intelligent Systems
SMASIS 2014
September 8-10, 2014, Newport, RI, USA**

SMASIS2014-#####

DEVELOPMENT AND CHARACTERIZATION OF EMBEDDED SENSORY PARTICLES USING MULTI-SCALE 3D DIGITAL IMAGE CORRELATION

Stephen R. Cornell
Texas A&M University
College Station, TX 77840

William P. Leser
NASA Langley Research Center
Hampton, VA 23681

Jacob D. Hochhalter
NASA Langley Research Center
Hampton, VA 23681

John A. Newman
NASA Langley Research Center
Hampton, VA 23681

Darren J. Hartl
Texas A&M University
College Station, TX 77840

ABSTRACT

A method for detecting fatigue cracks has been explored at NASA Langley Research Center. Microscopic NiTi shape memory alloy (sensory) particles were embedded in a 7050 aluminum alloy matrix to detect the presence of fatigue cracks. Cracks exhibit an elevated stress field near their tip inducing a martensitic phase transformation in nearby sensory particles. Detectable levels of acoustic energy are emitted upon particle phase transformation such that the existence and location of fatigue cracks can be detected. To test this concept, a fatigue crack was grown in a mode-I single-edge notch fatigue crack growth specimen containing sensory particles. As the crack approached the sensory particles, measurements of particle strain, matrix-particle debonding, and phase transformation behavior of the sensory particles were performed. Full-field deformation measurements were performed using a novel multi-scale optical 3D digital image correlation (DIC) system. This information will be used in a finite element-based study to determine optimal sensory material behavior and density.

1 Introduction

Knowledge of fatigue cracks in aerospace materials is a major concern in the long-term use of aircraft. Currently, aircraft undergo routine overhauls at specified intervals during the lifetime of the vehicle in which major dismantling occurs, followed by detailed part-by-part inspection for fatigue cracking (c.f. Nechval et al. (2011)). Using methods for sensing compositional changes in embedded active-material particles, sensory particles, as a method for non-destructive evaluation (NDE) is proposed for giving real-time sensing of fatigue crack growth in key structural members of an aircraft which are susceptible to fatigue. This NDE method is intended to alleviate the need for frequent dismantling of aircraft, as well as to provide a live status update on the presence of fatigue cracks in the aircraft components.

Figure 1 provides an illustration of the sensory particle concept. A sensory particle located near the crack tip has a response (mechanical, acoustic, magnetic, resistive) to the intensified stress field which can be detected using existing NDE methods. Various material systems may be used as sensory particles, allowing various NDE sensing methods to be incorporated. Some possible NDE methods include acoustic sensing of phase transformation in shape memory alloys (SMAs, e.g., NiTi) (Bogdanoff and Fultz, 2001), magnetic sensing of reorientation of martensitic variants in magnetic shape memory alloys (MSMAs, e.g., *NiMnGa*) (Karaca et al., 2006), or detection of changes in resistance of piezoelectric materials (e.g.,$BaTiO_3$) (Hiruma et al., 2004). In the present work, the NiTi shape memory alloy (SMA) was used as the sensory particle material, which emits an acoustic signal upon the onset of stress-induced martensitic

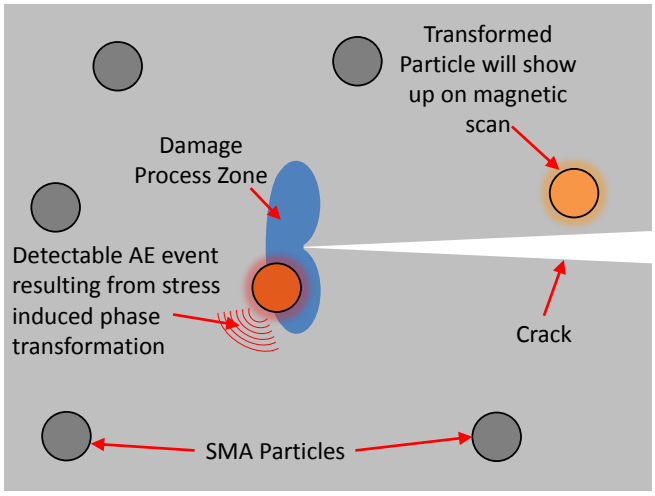

FIGURE 1. A schematic of the sensory particle concept. Various types of sensory particles may be used, including SMAs, MSMAs, or piezoelectrics.

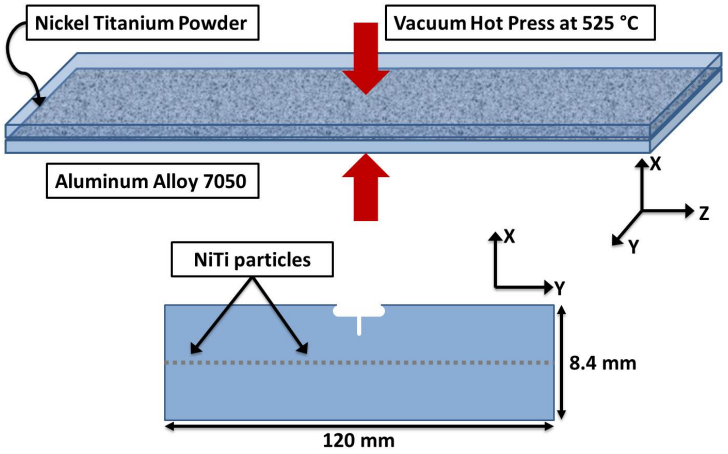

FIGURE 2. Schematic of hot-pressing and machining of test specimens.

phase transformation.

Development of the sensory particle concept relies on the use of advanced material modeling methods. Calibration of the constitutive model parameters must be performed through iterative comparison between experimental full-field measurement results and simulation. The strain measurements performed in this work are intended to provide detailed information for calibration. Mode-I loading of fatigue pre-cracked single-edge notch (SEN) specimens was used to generate data for calibration, and provide a first-step analysis of the behavior of the sensory particle and matrix material in the presence of a fatigue crack.

3D digital image correlation (3D-DIC) was used in these experiments to measure the full-field strain distribution on the surface of the specimens. This technique utilizes optical discontinuities to track the displacements, both in and out of plane, at many different points on the specimen surface during a test. For DIC, the surface of a specimen must have a random distribution of visual discontinuity, or speckle pattern. If the material being tested does not have a naturally occurring speckle pattern, one must be applied using one of many possible speckling techniques (Sutton et al.).

Speckle patterning can be performed in many different ways for different applications. For this work, a speckle pattern was applied at both the micro- and macro- scales. Creating a speckle pattern at the microscale is especially challenging; Kammers and Daly (2011) reviewed several techniques for speckle patterning at a microscale. Some techniques include nanoparticle surface deposition (this method was used with an optical stereo-microscope) (Berfield et al., 2007), chemical vapor deposition (Scrivens et al., 2007), and e-beam lithography (Li et al., 2011). For macroscale patterning of metallic materials, spray paint speckle-patterning is commonly used (Sutton et al.).

2 Experimental method

Specimens were fabricated using aluminum alloy 7050 with embedded NiTi (50.9 atomic % Ni) shape memory alloy (SMA) particles. Aluminum alloy 7050 is a common aerospace structural material which was identified as being of particular interest for the sensory particle concept. Figure 2 is a diagram that shows the fabrication technique for creating the material specimens with embedded NiTi particles. 100 μm-diameter gas atomized NiTi particle spheres were scattered onto an aluminum alloy 7050 plate. A second aluminum plate was placed on top of the particle bed, and the plates were vacuum hot-pressed at 525 ^{o}C and 35 MPa for 1 hour to create the bulk panel. The panel was solutionized at 490 ^{o}C for 6 hours and peak aged at 121 ^{o}C for 24 hours in vacuum. The mechanical properties of the aluminum matrix material were measured to be $E = 80$ GPa and $\sigma_y = 425$ MPa. Figure 2 illustrates the SEN specimens that were cut from the cross-section of the hot-pressed panel by electrical discharge machining (EDM). Consequently, the sensory particles were aligned along the center-line of the specimen.

The experiments presented in this section mimic application of sensory particles to provide proof of concept. Before testing the specimen with 3D-DIC at multiple scales, the specimen was pre-cracked up to 200 μm from the interface of NiTi particles. This was accomplished by fatigue cycling at a stress intensity factor of $K_{max} = 7.25$ MPa$\sqrt{\text{m}}$, load ratio $R = 0.1$, and frequency of 20 Hz. The resulting crack length was 4.0 mm.

The fatigue pre-cracked SEN specimen was prepared for DIC using two different speckle pattern techniques. E-beam lithography was applied to the specimen such that the pattern covered one or more NiTi particles (Gupta et al., 2014). This pat-

tern was applied over a 2 mm^2 area with 2 μm diameter speckles. Figure 3 shows the microscale speckle pattern applied for this work. Next, a macroscopic speckle pattern was applied to the entire specimen by first masking the microscale speckle pattern using tape then applying a spray paint macroscale speckle pattern. For the macroscale DIC measurements, the entire specimen surface was prepared by first spray painting a white background on the specimen with sufficient thickness to circumvent reflection of light from the metallic specimen surface. Subsequently, a random pattern of black spray paint speckles was applied to the specimen surface. It should be noted that the lighting should be optimized for speckle pattern contrast.

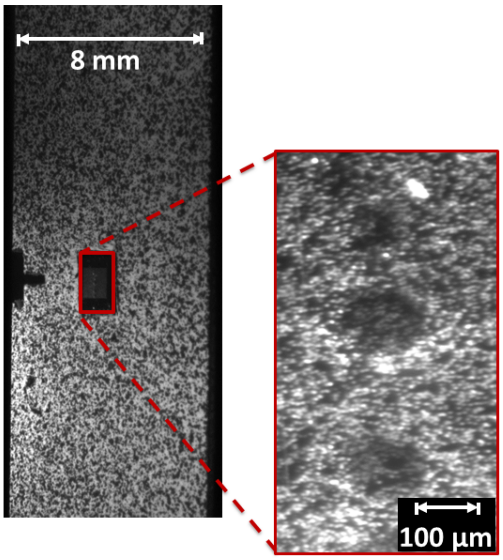

FIGURE 3. Speckle patterns applied to the specimen. The spherical NiTi particles can be seen inside the aluminum alloy 7050 matrix in the microscale image (right image).

Figure 4 shows the configuration of the stereo-microscope and macroscale charge-coupled device (CCD) cameras with respect to the specimen. This configuration provides simultaneous 3D-DIC measurement of the macroscopic and microscopic deformations at the specimen level and within the sensory particles, respectively. For fatigue crack growth experiments, it is necessary to understand the deformation response of the material at the macroscale and near the specimen boundary conditions as the crack propagates through the material but also be able to analyze the behavior very near the crack tip and at a scale comparable to the size of the sensory particles ($\sim 100\ \mu$m). The macroscale measurements also provide boundary conditions for subsequent modeling efforts. Therefore, performing analysis at two different scales simultaneously is an important capability for this study.

Microscale measurements were performed using the VIC-3D Micro^{TM} system by Correlated Solutions, Inc. (2014). The 3D-DIC macroscale measurements were performed using two 5-megapixel CCD cameras with 23 mm lenses. The macroscale cameras were attached on either side of the stereo-microscope in a plane parallel to the isolation optical table. The stereo-microscope has a fixed focal length; therefore, with the specimen placed in the test stand grips, the image for the stereo-microscope was focused after which the image for the macroscale cameras was focused. The maximum magnification that can be achieved using the stereo-microscope is 11.8x magnification with a field of view (FOV) of 1 mm^2, which was the magnification used in the experiments described herein.

A 15 kN load cell was used with wedge grips for the crack growth specimen load-to-failure test. The table-top test stand and DIC setup was placed on an optical isolation table to minimize vibrations in the DIC measurements. The test was performed under stroke control at 0.05 mm/s. A single over-load cycle was applied to the fatigue pre-cracked SEN specimen such that $K_{max} = 39.1$ MPa$\sqrt{\text{m}}$ and unloaded, over a period of 600 seconds. Images were obtained during the over-load cycle at 1 Hz, and captured using a software-trigger in VIC-Snap^{TM} (Correlated Solutions, Inc., 2014) such that all four cameras captured images simultaneously.

3 Results

3.1 Macroscale 3D-DIC results

Figure 5 illustrates strain fields measured at six different times during the over-load cycle. Figure 5(a) shows the times

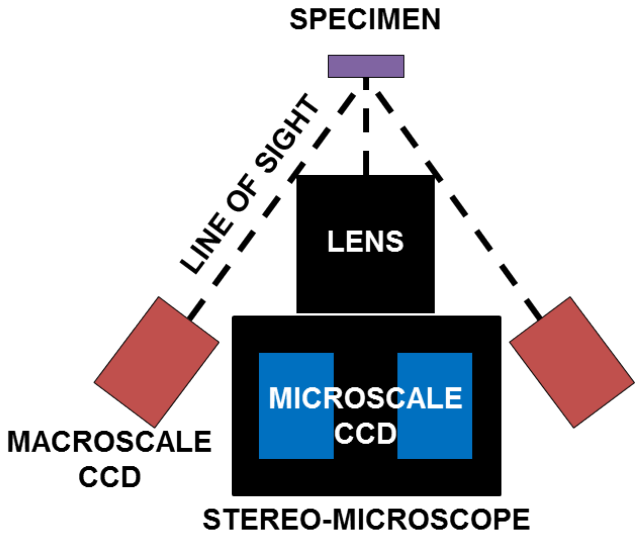

FIGURE 4. Orientation of multi-scale 3D-DIC system (4 cameras total).

when the images were selected and Figure 5(b) shows the axial strain contours (ε_y) in the specimen. The images in Figure 5(b) correspond to the numbered points in Figure 5(a). Crack propagation occurred between images 2 and 3. The effect of the propagation can be seen in these images. Displacements can be extracted along the lines that form the boundary of the images and applied as constraints to a corresponding FE model.

3.2 Microscale 3D-DIC results

The microscale 3D-DIC axial strain measurements within the sensory particles of interest, near the crack tip, are shown in Figure 6. Figure 6 shows the contour fields of axial strain (ε_y) in the specimen close to the crack tip corresponding to the time points shown in Figure 5(a). The area of interest (AOI) for the DIC analysis was chosen just below the crack tip, and included two sensory particles and the surrounding matrix material. Additionally, DIC results could only be obtained for the bottom portion of the sensory particle closest to the crack tip because of poor DIC correlation. Future experiments will explore methods for improving DIC correlation on a particle and increasing DIC resolution. A second particle farther from the crack tip was also included in this AOI. The AOI was selected below the crack tip because of poor correlation in the area closer to the crack tip.

Image 1 in Figure 6 shows the axial strain (ε_y) field before the peak load. Image 2 followed by image 3 demonstrates the effect of crack propagation on the measured strain field. Image 4 shows the ε_y contours at the peak applied load during the experiment, which was 1415 N. Images 5 and 6 show the ε_y contours during unloading.

Figure 7 demonstrates the strain behavior at two particles near the crack tip. As seen in Figure 7(a), Particle 1 is very close to the crack tip (indicated by the red line), while Particle 2 is farther from the crack tip. The blue and red dots are the points at which local strain measurements were extracted in Figure 7(b). It can be seen from Figure 6 that between images 2 and 3 a sharp change in strain occurred, which is associated with the crack propagation event mentioned previously. At the same load in Figure 7, it is seen that a corresponding sharp increase in strain occurred in Particle 1 (blue line in Figure 7). This sharp change in particle behavior indicates martensitic phase transformation. Phase transformation did not occur in Particle 2.

This brief analysis of the sensory particle transformation in the presence of a crack demonstrates the importance of modeling to fully understand the observed behavior. To calibrate the constitutive model parameters of the sensory particles, comparison of a simulation to the experimental strain results is still needed. It is expected that by reproducing this experiment in a simulation, the fundamental behavior of the sensory particles can be understood.

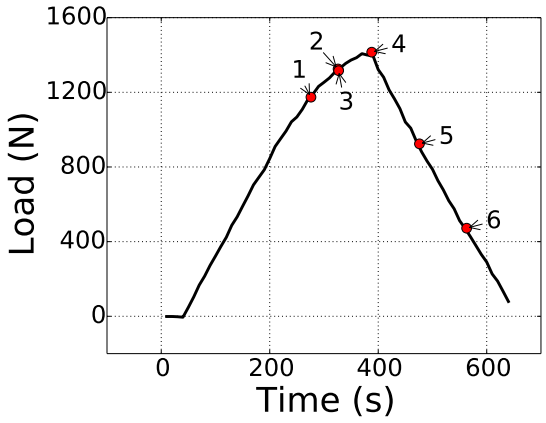

(a)

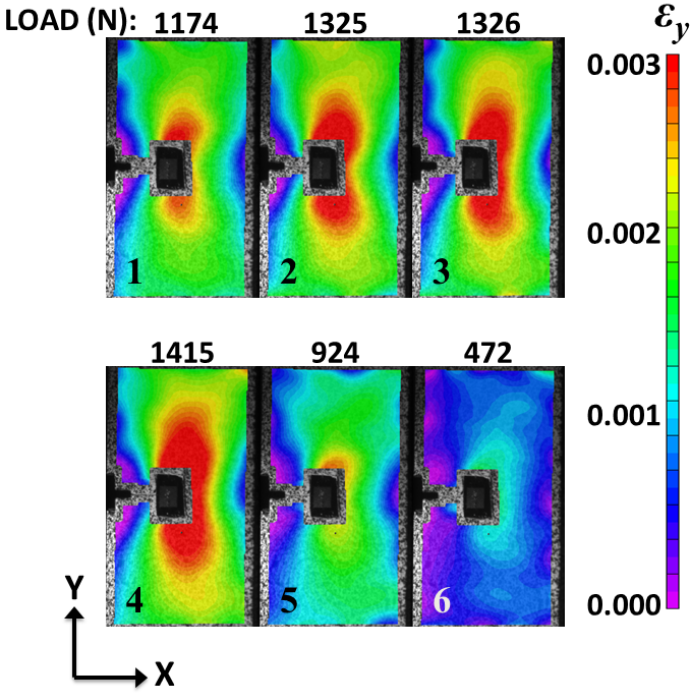

(b)

FIGURE 5. (a) Externally applied load vs time plot showing the times when the DIC images were selected, and (b) 3D-DIC full-field axial strain (ε_y) macroscale results.

4 Summary and conclusions

The key features of this work may be summarized in the following points:

1. A novel method for deformation measurement at multiple scales has been explored, which utilizes the 3D-DIC full-field measurement technique. Microscopic 3D-DIC was per-

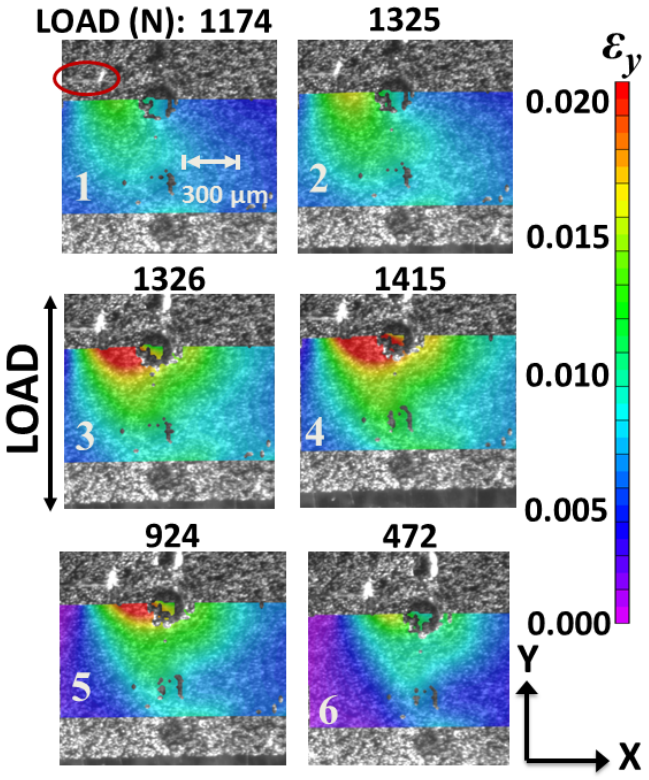

FIGURE 6. Microscale 3D-DIC axial strain (ε_y) results surrounding the crack at time points shown in Figure 5(a). The crack location is indicated by the red circle.

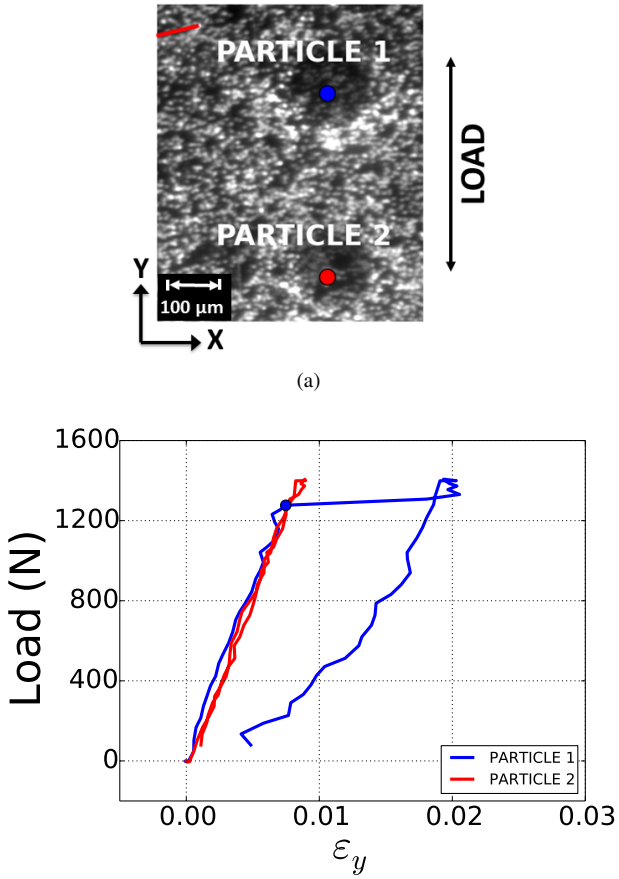

FIGURE 7. (a) Analysis point chosen in Particle 1 and location of the crack (red line), and (b) axial strain (ε_y) response at that analysis point.

formed through a stereo-microscope simultaneously with a standard macroscopic 3D-DIC setup.

2. The sensory particle concept was explored further by single-cycle tensile loading of a fatigue crack growth sensory particle specimen. The material specimen consisted of gas atomized NiTi (50.9 atomic % Ni) as the sensory material surrounded by aluminum alloy 7050 matrix. Using the 3D-DIC setup, sensory particle transformation was detected near the growing fatigue crack.

This work has introduced crack growth experimentation for the sensory particle concept. The purpose of performing these experiments is primarily to provide a proof of concept and to improve the fidelity of future modeling. High fidelity models of sensory particle crack growth specimens are currently being obtained from x-ray computed tomography (CT) and should be used in an attempt to replicate measured results. In addition to being able to calibrate the material parameters for the model, these studies will be able to provide a more rigorous analysis of the sensory particle concept. Future experiments will explore the effect of high-cycle fatigue. Additionally, studies should be performed to explore alternative sensory particle materials and NDE methods.

REFERENCES

Berfield, T., Patel, J., Shimmin, R., Braun, P., Lambros, J., and Sottos, N. (2007). Micro-and nanoscale deformation measurement of surface and internal planes via digital image correlation. *Experimental Mechanics*, 47:51–62.

Bogdanoff, P. and Fultz, B. (2001). The role of phonons in the thermodynamics of the martensitic transformation in NiTi. *Philosophical Magazine B: Physics of Condensed Matter; Statistical Mechanics, Electronic, Optical and Magnetic Properties*, 81:299 – 311.

Correlated Solutions, Inc. (2014). www.correlatedsolutions.com.

Gupta, V. K., Willard, S. A., Hochhalter, J. D., and Smith, S. W. (2014). Microstructure-scale in-situ correlation-based study of grain deformation and crack tip displacements in al-cu alloys.

Materials Performance and Characterization, In Review.

Hiruma, Y., Aoyagi, R., Nagata, H., and Takenaka, T. (2004). Piezoelectric properties of $BaTiO_3 - (Bi_{1/2}K_{1/2})TiO_3$ ferroelectric ceramics. *Japanese Journal of Applied Physics, Part 1: Regular Papers and Short Notes and Review Papers*, 43:7556 – 7559.

Kammers, A. and Daly, S. (2011). Small-scale patterning methods for digital image correlation under scanning electron microscopy. *Measurement Science and Technology*, 22:125501.

Karaca, H., Karaman, I., Basaran, B., Chumlyakov, Y., and Maier, H. (2006). Magnetic field and stress induced martensite reorientation in NiMnGa ferromagnetic shape memory alloy single crystals. *Acta Materialia*, 54:233 – 245.

Li, N., Guo, S., and Sutton, M. A. (2011). Recent progress in e-beam lithography for SEM patterning. In *MEMS and Nanotechnology, Volume 2*, pages 163–166. Springer.

Nechval, N., Nechval, K., Purgailis, M., and Strelchonok, V. (2011). Planning inspections in the case of damage tolerance approach to service of fatigued aircraft structures. *International Journal of Performability Engineering*, 7.

Scrivens, W., Luo, Y., Sutton, M., Collette, S., Myrick, M., Miney, P., Colavita, P., Reynolds, A., and Li, X. (2007). Development of patterns for digital image correlation measurements at reduced length scales. *Experimental Mechanics*, 47:63–77.

Sutton, M. A., Orteu, J.-J., and Schreier, H. W. *Image correlation for shape, motion and deformation measurements: basic concepts, theory and applications*. Springer, New York, NY (2009).